International Journal of Pharmaceutics 362 (2008) 163–171

Contents lists available at ScienceDirect

International Journal of Pharmaceutics

journal homepage: www.elsevier.com/locate/ijpharm

Pharmaceutical Nanotechnology

Evaluating particle hardness of pharmaceutical solids using AFM nanoindentation

Victoria M. Masterson, Xiaoping Cao*

Pfizer Global Research & Development, Eastern Point Road, Groton, CT 06340, United States

ARTICLE INFO

Article history:
Received 9 April 2008
Received in revised form 10 June 2008
Accepted 11 June 2008
Available online 26 June 2008

Keywords:
Atomic force microscopy
Nanoindentation
Particle
Hardness
Pharmaceutical solids

ABSTRACT

Understanding mechanical properties of pharmaceutical solids at the submicron scale can be very important to pharmaceutical research & development. In this paper, the hardness of individual particles of various pharmaceutical solids including sucrose, lactose, ascorbic acid, and ibuprofen was quantified using the atomic force microscopy (AFM) nanoindentation. Effects of data variation and indentation size or peak load on hardness are evaluated. The results show acceptable reproducibility and indicate that data variation may be primarily from the inhomogeneous nature of the samples. Different extents of indentation size or peak load effect on hardness were observed for the samples. With consideration of both data variation and indentation size effects, the hardness values of different samples were compared at similar contact depths or peak loads. The hardness ranked as: ascorbic acid > sucrose > lactose ≈ ibuprofen, at contact depths from ~40 to 400 nm or peak loads ranging from ~16 to 70 μN. Additionally, the potential implication of particle hardness to compact hardness and tableting performance was discussed.

1. Introduction

Mechanical properties of pharmaceutical solids play an important role in pharmaceutical research & development including solid dosage form design and manufacturing, particle size control, and excipient selection (Amidon, 1995; Hiestand, 1997; Hancock et al., 2001; Sun and Grant, 2001; Mullarney and Hancock, 2006). Commonly, the mechanical properties have been determined by bulk methods such as impact-rebound (Hiestand et al., 1971) and beam-bending (Podczeck, 2001). These methods are performed on compacts made from the powders. Complicated sample preparations, demand for relatively large sample size and time-consuming procedures limit their use in pharmaceutical industry. Other drawbacks of these bulk methods include the influence of porosity (Hancock et al., 2000), particle size and shape (Hancock et al., 2001), and potential changes in mechanical properties due to the compaction process, resulting in large variations in reported data.

In the last two decades, effort has been made in the development of techniques for probing the mechanical properties of materials at the submicron scale (Oliver and Pharr, 1992; Rowe and Roberts, 1995; Fraxedas et al., 2002). These techniques, especially nanoindentation, allow indentation measurements to be conducted on individual particles or crystals (Taylor et al., 2004a,b). With the rapid development of atomic force microscopy (AFM), AFM nanoindentation has quickly become a very promising technique to assess mechanical properties at a nanometer scale. It allows a unique combination of high-resolution imaging, composition mapping with spatial resolution in nanometers and local mechanical studies with forces at nanoNewtons (Vanlandingham et al., 1997; Belikov et al., 2007).

Recently, AFM nanoindentation studies have been employed to study pharmaceutical materials such as lactose (Perkins et al., 2007), sucrose (Liao and Wiedmann, 2004; Ramos and Bahr, 2007), sodium stearate (Liao and Wiedmann, 2004), acetaminophen (Liao and Wiedmann, 2004, 2005) and sulfathiazole (Picker-Freyer et al., 2007). These studies reported some particle hardness data and showed potential applications of AFM nanoindentation to pharmaceutical research. However, some of the studies differed largely in experimental measurements and result analysis, making it difficult to compare the hardness results from different studies. In addition, very limited discussion was found for effects of data variation and indentation size or peak load that may significantly affect the hardness value and comparison. In this paper, the hardness of individual particles was quantified for pharmaceutical solids including sucrose, lactose, ascorbic acid and ibuprofen using AFM nanoindentation. With consideration of both data variation and indentation size or peak load effects, the hardness of different samples was compared. Additionally, the potential implication of particle hardness to compact hardness and tableting performance was discussed.

* Corresponding author. Tel.: +1 860 686 1260; fax: +1 860 441 3972.
E-mail address: xiaoping.cao@pfizer.com (X. Cao).

0378-5173/$ – see front matter © 2008 Elsevier B.V. All rights reserved.
doi:10.1016/j.ijpharm.2008.06.015

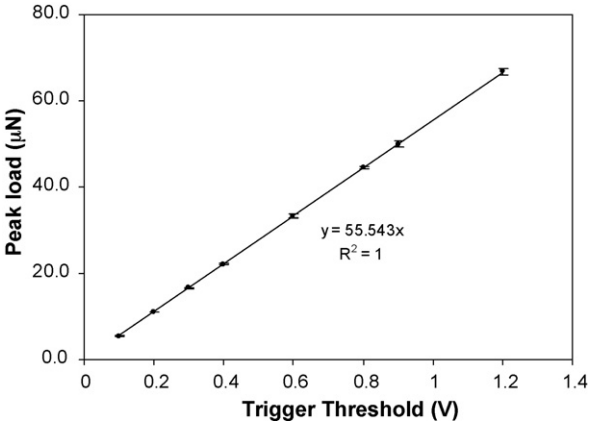

Fig. 1. The peak load as a function of the trigger threshold during AFM nanoindentation.

2. Materials and methods

2.1. Materials and sample preparations

The lactose (316 Fast Flo, spray dried) was obtained from Foremost Farm (Philadelphia, PA). The sucrose was purchased from Sigma Aldrich with a 99.5% purity. The sucrose crystals were washed with methanol to remove small crystallites on the surfaces and produce a smooth surface suitable for AFM nanoindentation experiments. The ascorbic acid was obtained from ScienceLab with a 99.0%+ purity. The ibuprofen with a particle size (volume mean diameter) of ~90 μm was obtained from BASF Corporations (Ibuprofen 90). To prepare the particle samples for AFM nanoindentation, a thin layer of epoxy (Loctite Medical Epoxy, M-21HP, Hysol®) was cast on a glass coverslip substrate, and the sample particles were then fixed on the epoxy film. Only the sucrose crystals were large enough to be handled individually and were placed on the epoxy film with the largest crystal face exposed for nanoindentation. The lactose, ascorbic acid and ibuprofen particles were dispensed carefully on the epoxy film using a spatula. After the epoxy film was allowed to harden for about 45 min, the excess particles were removed by lightly tapping the glass cover slip on its side.

2.2. AFM nanoindentation

A Nanoscope IIIa Multimode AFM (Veeco Metrology Group, Santa Barbara, CA) was used to analyze all samples. The experiments were performed in air at ambient conditions. A JV-type scanner (Veeco Metrology Group, Santa Barbara, CA) was used. A stainless steel cantilever with a cube corner pyramidal diamond tip (Veeco Probes, Santa Barbara, CA) was employed for both nanoindentation and imaging. The diamond tip had a length of 50 μm, a tip radius of curvature less than 50 nm, a contact sensitivity of 203 nm/V and a resonance frequency of about 64 kHz. Both height and phase images were collected and analyzed with Nanoscope software (Veeco). All images were collected with a resolution of 256 × 256 pixels, and majority of images were taken in a 2 μm × 2 μm scan area with a scan rate ranging from 0.4 to 1.0 Hz. The set point for the feedback control was between 0.14 and 0.37 V. The surface smoothness was evaluated by the mean roughness (R_a) that is defined as the average of the absolute values of surface height deviations from the mean plane. The mean roughness was calculated from the height image.

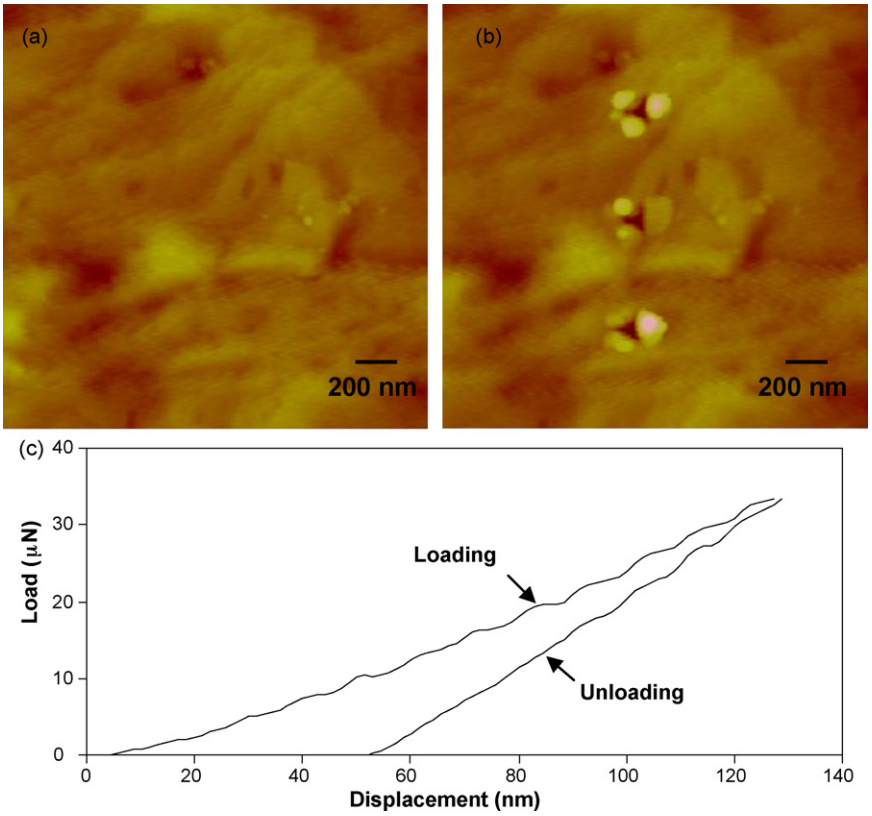

Fig. 2. AFM nanoindentation results of a sucrose crystal: (a) image before indentation; (b) image after indentation at a trigger threshold of 0.6 V. Both images have a Z scale of 80 nm. (c) A typical force curve at a trigger threshold of 0.6 V.

Table 1
Summary calculation results from multiple measurements for a sucrose crystal

Replicate	P_{max} (μN)	S (nN/nm)	h_c (nm)	H (GPa)
7	22.3 ± 0.1	487 ± 32	60 ± 6	2.4 ± 0.5
10	33.2 ± 0.1	500 ± 39	81 ± 13	2.0 ± 0.4
8	44.4 ± 0.3	514 ± 58	100 ± 14	1.8 ± 0.4

The standard deviations are included for each value.

For nanoindentation experiments, the set point was 0.9 V with trigger thresholds ranging from 0.1 to 1.2 V and threshold steps from 0.1 to 0.3 V. Different trigger thresholds generate different peak loads. Fig. 1 shows a plot of the peak load as a function of the trigger threshold. Multiple measurements for the same sample or different samples at the same trigger threshold indicated that the peak load is very reproducible with a relative standard deviation of <2%. The peak load is linearly proportional to the trigger threshold with a fitting coefficient (R^2) of 1. The indentation cycle was set to 1.0 Hz (one loading/unloading cycle per second), and no hold time was set at the peak load. Prior to nanoindentation the samples were imaged using a tapping mode with the diamond tip. During nanoindentation, the scan was stopped, and the tip was positioned within the scan area to make indents. Force curves were recorded for each indent. Immediately after indentation was complete, the same area was imaged again with the diamond tip using a tapping mode. In order to ensure the indentations were representative of the sample, usually multiple sets of indentations were made at different locations of the sample.

The AFM nanoindentation experiments for sucrose, lactose, ascorbic acid and ibuprofen were performed on single particles. Since the epoxy film was used in particle sample preparations, the images and indentation characteristics of the epoxy film were obtained as a control prior to experiments on single particle samples. This approach ensured that the indentation actually took place on the samples of interest because the single particle samples exhibited very different surface morphology and indentation characteristics from the epoxy film.

2.3. Data analysis

The Oliver-Pharr method was used for calculations (Oliver and Pharr, 1992). The hardness (H) can be calculated using the following equation.

$$H = \frac{P_{max}}{A_c} \quad (1)$$

where P_{max} is the indentation peak load and A_c is the contact area between the indenter and surface. The peak load can be directly obtained from the force curve generated during indentation. For a cubed corner indenter, the contact area (A_c) is estimated from the contact depth (h_c) using the following equation (Durst et al., 2006).

$$A_c = 2.598h_c^2 \quad (2)$$

The contact depth (h_c) is calculated from the peak load (P_{max}), stiffness (S) and maximum indenter displacement (h_{max}) using the following equation.

$$h_c = h_{max} - \varepsilon\left(\frac{P_{max}}{S}\right) \quad (3)$$

The h_{max} can be determined from the unloading curve, and S is estimated from the slope of the top one third portion of the unloading curve (Doerner and Nix, 1986). The geometric constant ε is equal to

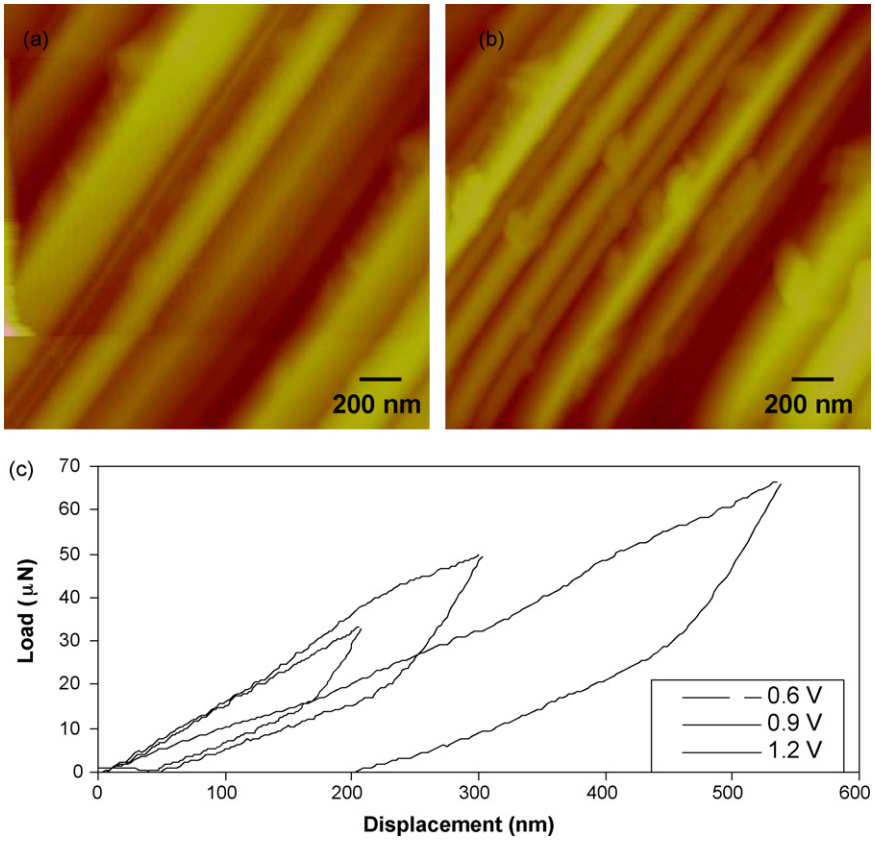

Fig. 3. AFM nanoindentation results of a lactose particle: (a) image before indentation; (b) image after indentation at trigger thresholds of 0.6, 0.9 and 1.2 V. Both images have a Z scale of 400 nm. (c) Typical force curves at trigger thresholds of 0.6, 0.9 and 1.2 V.

Table 2
Summary calculation results from multiple measurements for a lactose particle

Replicate	P_{max} (μN)	S (nN/nm)	h_c (nm)	H (GPa)
3	33.1 ± 0.2	408 ± 48	167 ± 42	0.51 ± 0.22
3	49.1 ± 0.5	438 ± 33	212 ± 20	0.43 ± 0.08
3	66.1 ± 0.3	450 ± 56	378 ± 43	0.18 ± 0.04

The standard deviations are included for each value.

0.72 for conical and pyramidal indenters (Oliver and Pharr, 1992), which is the value used in the calculations of this study.

To verify the above area function, over 30 indents were generated on a homogeneous HPMC film at various peak loads. The contact areas of the indents were obtained from the AFM image using Nanoscope software (Veeco), and the contact depths were calculated using Eq. (3). An area function was derived by empirically fitting a function to a plot of the imaged areas versus the contact depths. It was found that the area function stated in Eq. (2) is in reasonable agreement with the fitted area function. In most cases it is difficult to accurately determine the contact area by AFM imaging due to surface features near the indents such as material pileup and sink-in, resulting in large variations in the imaged areas of the indents generated at the same peak load. Therefore, all contact area values in this study were calculated using Eq. (2).

3. Results

3.1. Sucrose

Fig. 2 shows AFM nanoindentation results for a sucrose crystal. The indentation was conducted with a trigger threshold of 0.6 V in triplicate. Fig. 2a shows a height image of the crystal surface before indentation. The image revealed fine surface features such as protrusions and depressions and indicated a mean surface roughness of ~10 nm. Three triangular indents with a similar size were generated after indentation, and material pileup near the indents was observed, as shown in Fig. 2b. A cross-sectional analysis indicates that the height of the pileup is ~20–25 nm. The amount of the pileup is related to intrinsic material properties as well as the indentation load and surface roughness. Experiments at different peak loads indicate more pileups were generated at larger peak loads. This is consistent with a previous observation on a sucrose crystal surface (Ramos and Bahr, 2007). Additionally, the lateral extent of the pileup shows a plastic deformation mechanism of the sucrose crystal. The presence of the pileup without any observed cracking suggests that the sucrose material was able to flow to the sample surface from beneath the indenter via a dislocation mechanism (Ramos and Bahr, 2007). During the indentation, force curves were recorded to determine peak loads, contact depth and hardness. Fig. 2c shows a typical force curve (load versus tip displacement) at a trigger threshold of 0.6 V. The force curve contains a loading and unloading curve. The corresponding peak load, stiffness, contact depth and hardness were determined to be ~33 μN, ~500 nN/nm, ~78 nm and ~2.0 GPa, respectively.

To investigate the indentation results at different peak loads and evaluate data reproducibility, experiments were performed at three trigger thresholds to obtain force curves at three peak loads, and 7–10 indents and measurements were conducted at each trigger threshold. Table 1 summarizes results for peak load (P_{max}), stiffness (S), contact depth (h_c) and hardness (H) with standard deviations. At the same peak load, 10–16% variation in contact depth was observed, and about 20% variation in hardness was observed

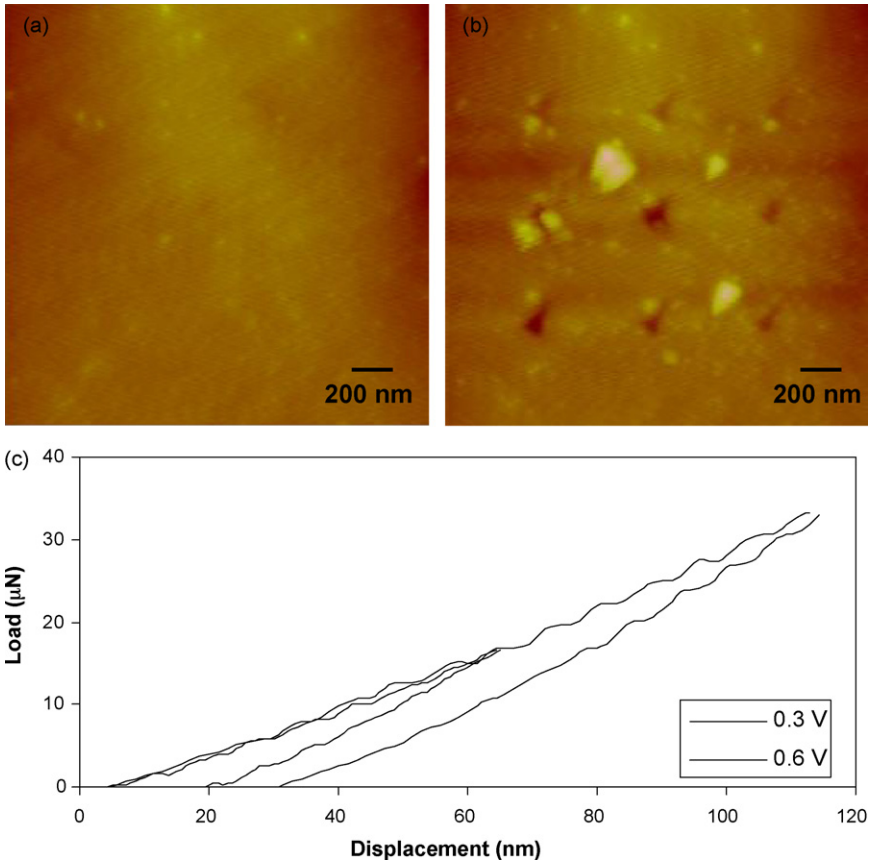

Fig. 4. AFM nanoindentation results of an ascorbic acid crystal: (a) image before indentation; (b) image after indentation with at thresholds of 0.3, 0.6 and 0.9 V. Both images have a Z scale of 100 nm. (c) Typical force curves at trigger thresholds of 0.3 and 0.6 V.

Table 3
Summary calculation results from multiple measurements for an ascorbic acid crystal

Replicate	P_{max} (μN)	S (nN/nm)	h_c (nm)	H (GPa)
3	16.7 ± 0.3	441 ± 14	38 ± 1	4.5 ± 0.2
6	33.5 ± 0.6	453 ± 5	49 ± 7	5.6 ± 1.8
6	50.3 ± 0.8	458 ± 11	65 ± 13	5.2 ± 2.7
3	67.3 ± 0.7	472 ± 2	69 ± 4	5.5 ± 0.7

The standard deviations are included for each value.

due to the variation of the contact depth. As the peak load increases from ~22 to 44 μN, the average contact depth increases from ~60 to 100 nm. No significant indentation size effect was observed in the 60–100 nm contact depth range due to the data variation, but the average hardness decreased slightly from ~2.4 to 1.8 GPa with the increase of the contact depth. The values agree reasonably well with previously reported hardness values of 636 MPa (Ridgway et al., 1969), 1.5 GPa (Ramos and Bahr, 2007) and 6560 MPa (Liao and Wiedmann, 2004). The spread of the data can be attributed to different instrumentation, measurement scale and possible indentation size effect.

3.2. Lactose

Fig. 3 shows AFM nanoindentation results for a lactose particle at trigger thresholds of 0.6, 0.9 and 1.2 V. The surface before indentation exhibited a line-texture morphology with protrusions and depressions, as shown in Fig. 3a. The surface was rough with the largest height difference on surface of over 160 nm and a mean roughness of ~31 nm. Surprisingly, no obvious indents were observed after the indentation, as shown in Fig. 3b. The surface morphology after indentation only appeared to be slightly different from that before indentation, and the line-texture morphology appeared to be more pronounced with an increased average roughness of ~33 nm. Additionally, some pileup was observed on surface after indentation. One possible reason for the lack of visible indents is due to the rough surface of the lactose particle. The tall protrusions and deep depressions on surface may prohibit the diamond tip from capturing possible indents. Note that the images were captured with the diamond tip immediately after indentation to ensure the same area was imaged. The diamond tip may not give as good resolution as conventional imaging tips such as silicon nitride or silicon tips. In addition, large extent of elastic recovery of the lactose particle after indentation (discussed below) may also cause the indents less obvious. Another possible reason for the lack of visible indents is that the lactose is a very brittle material (Narayan and Hancock, 2003) and the indentation may have created surface breakage rather than indent, resulting in increased surface texture and material pileup.

Although the indents were not observed, the force curves were generated, as shown in Fig. 3c. The corresponding peak loads were ~33, 49 and 66 μN. Compared with sucrose, the force curve of lactose appears to be smoother, and the unloading curves have less steep slopes. A small slope of the unloading curve suggests that the lactose particle underwent a large extent of elastic recovery upon unloading. This observation is consistent with a previous study for single crystals of alpha monohydrate lactose (Perkins et al., 2007). The calculated results for stiffness (S), contact depth (h_c) and hardness (H) are summarized in Table 2. The stiffness values appeared to increase slightly with the increase of the peak load, and the contact depth increased with the increase of the peak load. About 10–25% variation in contact depth was observed at the same peak load,

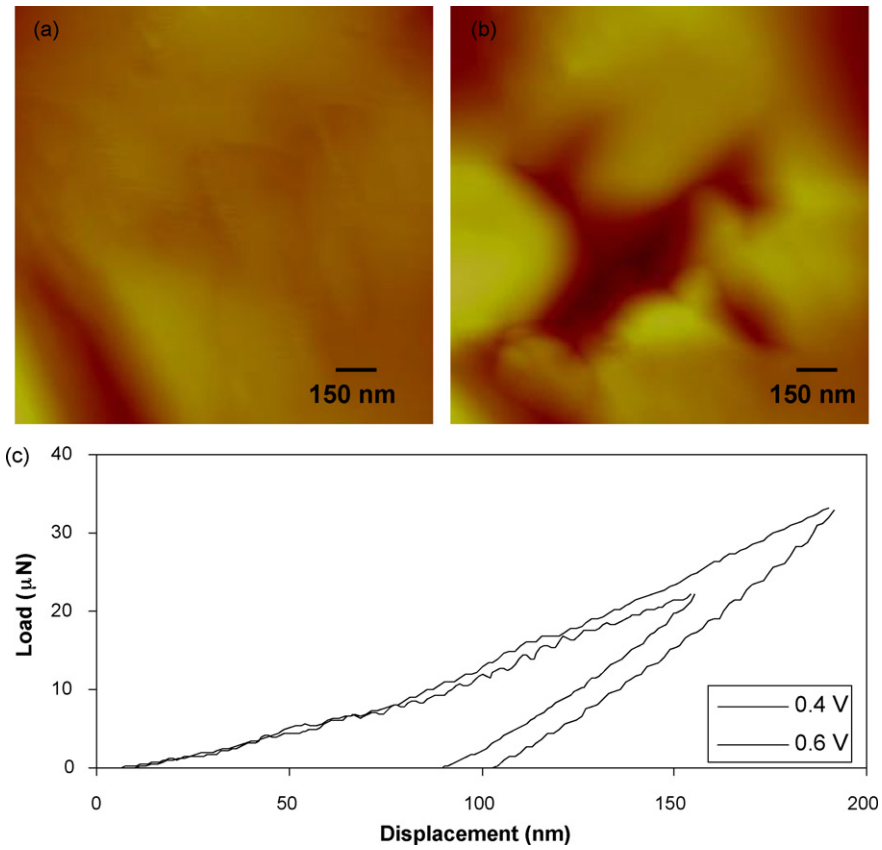

Fig. 5. AFM nanoindentation results of an ibuprofen crystal: (a) image before indentation; (b) image after indentation at trigger thresholds of 0.4 and 0.6 V. Both images have a Z scale of 300 nm. (c) Typical force curves at trigger thresholds of 0.4 and 0.6 V.

Table 4
Summary calculation results from multiple measurements for an ibuprofen crystal

Replicate	P_{max} (μN)	S (nN/nm)	h_c (nm)	H (GPa)
3	22.0 ± 0.1	432 ± 23	101 ± 21	0.9 ± 0.4
2	33.0 ± 0.1	468 ± 27	167 ± 40	0.5 ± 0.2

The standard deviations are included for each value.

Table 5
Summary calculation results from multiple measurements for a HPMC film

Replicate	P_{max} (μN)	S (nN/nm)	h_c (nm)	H (GPa)
3	5.5 ± 0.1	374 ± 26	40 ± 1	1.32 ± 0.02
3	11.1 ± 0.0	416 ± 20	54 ± 1	1.47 ± 0.06
3	16.5 ± 0.3	476 ± 7	74 ± 2	1.17 ± 0.05

The standard deviations are included for each value.

resulting 20–40% variation in hardness. Since the lactose (316 Fast Flo, spray dried) sample used in this study is a mixture of crystalline and amorphous lactose, the inhomogeneous nature of the sample is probably the cause of the variations in contact depth and hardness at the same peak load. Although relatively large variations in hardness were exhibited, the indentation size effect on hardness was still observed. As shown in Table 2, the average hardness values decreases from ~0.51 to 0.18 GPa when the contact depth increases from ~167 to 378 nm. A similar size effect was observed in a previous study for pure alpha monohydrate lactose when the probes with different radii were used (Perkins et al., 2007).

3.3. Ascorbic acid

Fig. 4 shows AFM nanoindentation results for an ascorbic acid crystal at trigger thresholds of 0.3, 0.6 and 0.9 V. The AFM height image before indentation, as shown in Fig. 4a, indicates that the surface of the ascorbic acid crystal before indentation was smooth with a mean roughness of ~5 nm. The indentation was carried out at the three trigger thresholds to generate the first row with three indents, and was repeated two more times at same thresholds to generate a 3 × 3 array of indents, as shown in Fig. 4b. The three indents in the right, middle and left columns were produced at thresholds of 0.3, 0.6 and 0.9 V, respectively. Material pileup was observed near most of the indents. It appears that larger pileups were created at larger trigger thresholds. Further examination shows that one indent was almost buried by the pileup and some pileups were present in between the indents. This is probably because the tip moved the pileups during the imaging after indentation. Fig. 4c shows typical force curves at the trigger thresholds of 0.3 and 0.6 V. The peak loads associated with the two trigger thresholds were ~17 and 33 μN, respectively. When compared with sucrose and lactose, the force curves of the ascorbic acid and sucrose are not as smooth as those of the lactose.

Table 3 summarizes the results for peak load (P_{max}), stiffness (S), contact depth (h_c) and hardness (H) from multiple measurements at trigger thresholds of 0.3, 0.6, 0.9 and 1.2 V. Multiple measurements at the same peak load showed 2–20% variation in contact depth, but in general, the contact depth increased with the increase of the peak load. As the peak load increased from ~17 to 67 μN, the average contact depth increased from ~38 to 69 nm. The contact depth of ascorbic acid was much smaller when compared with those of sucrose and lactose at the same peak load. For example, at a peak load of ~33 μN, the contact depths of ascorbic acid, sucrose and lactose were ~49, 81 and 167 nm, respectively. About 5–50% variation in hardness was observed due to the variation in contact depth. In the contact depth range of 40–70 nm, no significant indentation size effect on hardness was observed and the average hardness value was ~5.2 GPa.

3.4. Ibuprofen

Fig. 5 shows AFM nanoindentation results for an ibuprofen crystal at trigger thresholds of 0.4 and 0.6 V. The AFM height images show that the surface of the ibuprofen crystal had a mean roughness of ~10 nm before indentation and ~26 nm after indentation. In addition to the four indents and some material pileup near the indents, material sink-in was observed in between the indents. Fig. 5c shows typical force curves at trigger thresholds of 0.4 and 0.6 V. The peak loads associated with the two trigger thresholds were ~22 and 33 μN, respectively. Table 4 summarizes the calculation results for peak load (P_{max}), stiffness (S), contact depth (h_c) and hardness (H). As the peak load increased from ~22 to 33 μN, the average contact depth increased from ~101 to 167 nm. About 20% variations in contact depth were observed for multiple measurements at the same peak load, resulting ~50% variations in hardness. It is difficult to assess the indentation size effect due to the overlap in data variation, but the average hardness values decreases from ~0.9 to 0.5 GPa as the contact depth increases from ~101 to 167 nm. The observed surface features after indentation and calculated hardness suggests that the ibuprofen crystal is soft and brittle.

4. Discussion

To quantify and compare the particle hardness, data variations on hardness are first evaluated. During the experiments of this study, the peak load was controlled by the trigger threshold. It was observed that the peak load was very reproducible with <2% variation at the same trigger threshold, as shown in Fig. 1. However, 2–20% variation in contact depth at the same P_{max} was observed for the four materials, resulting in 5–50% variation in hardness. Possible causes of data variations include calculation method, instrumentation and sample characteristics. For the Oliver-Pharr method used for calculations in this study, the h_f/h_{max} ratio can be used to evaluate calculation accuracy on hardness determination, where h_f is the final depth of the indent (permanent deformation of the sample after complete unloading) and h_{max} is to the maximum tip displacement (tip displacement at peak load) (Bolshakov and Pharr, 1998; Pharr, 1998). It was found that when h_f/h_{max} is <0.7, the results from the Oliver-Pharr method agree well with that obtained from the finite element analyses (Bolshakov and Pharr, 1998) and the pileup or sink-in effect is not expected to significantly affect the results (Pharr, 1998). In this study, although the pileup and/or sink-in were observed for the four samples, the h_f/h_{max} ratios determined from the force curves were about 0.3–0.6. Therefore, the Oliver-Pharr method is appropriate for use to calculate hardness in this study.

To further evaluate possible causes of data variation, a smooth and homogenous hydroxypropyl methylcellulose (HPMC) film prepared by a spin-coating process (Lua et al., 2007) was employed for AFM nanoindentation experiments. The HPMC film had a mean surface roughness of <1 nm. Multiple measurements indicate <3% variation in contact depth and <5% variation in hardness at the same peak load, as shown in Table 5. The small data variations for the HPMC film suggest that the instrumentation is very reproducible for a smooth and homogenous sample. Therefore, data variations observed for the four materials may primarily rise from the inhomogeneous nature of the sample particles. First, since different surface roughness and surface features such as protrusions and depressions can impact the indentation results for particle samples, smooth areas were selected for nanoindentation using AFM imaging in order to reduce data variation. As discussed in a pre-

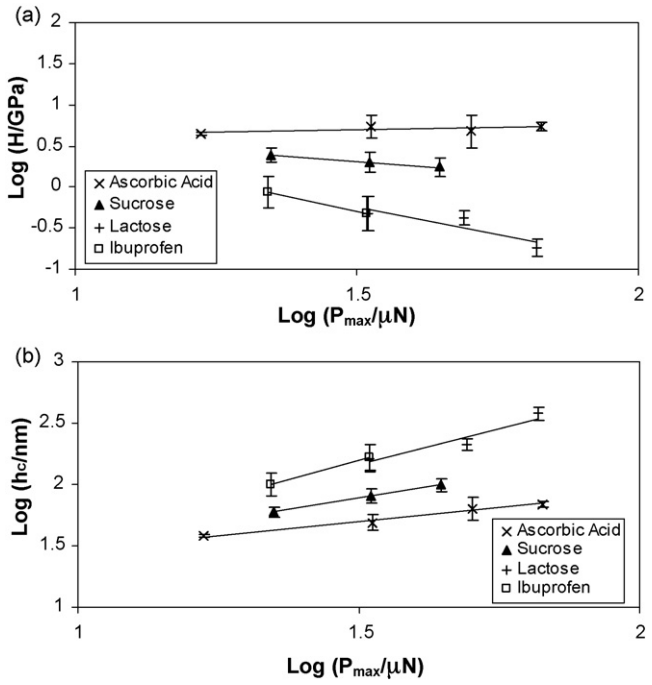

Fig. 6. Relationship among H, h_c and P_{max} for the four materials: (a) log(H) vs. log(P_{max}); (b) log(h_c) vs. log(P_{max}).

vious study (Liao and Wiedmann, 2004), the surface smoothness relates to sample treatment. In this study, the sucrose surface after methanol wash was found to be much smoother than the unwashed sample, and it was much easier to conduct indentation for the washed sucrose sample. The hardness was found to be similar for both samples, but the washed sucrose sample had smaller data variations. The lactose, ascorbic acid and ibuprofen samples were analyzed as they were, but effort was invested to identify a suitably smooth area for indentation. Although sample treatments may help to obtain smooth surface for indentation, care should be taken as treatments can potentially alter surface characteristics such as the hardness. A previous study showed that the hardness values of potassium chloride and acetaminophen were highly process-dependent (Liao and Wiedmann, 2005). Secondly, the dislocation density and presence of amorphous content in the sample can certainly introduce data variations for the small scale measurements like nanoindentation (Liao and Wiedmann, 2005; Ramos and Bahr, 2007). In addition, when different crystals of a same sample are analyzed, mixing of crystal facets can potentially affect the hardness measurements (Liao and Wiedmann, 2004; Ramos and Bahr, 2007). For example, a previous study for the sucrose crystals showed that the hardness of the (0 0 1) habit plane was different from that of the (1 0 0) by ~10% (Ramos and Bahr, 2007). Finally, the number of replicates at the same peak load may also affect the data variation. A previous study for the quenched potassium chloride showed that the hardness variation was up to ~45% sample at a peak load of 1000 μN when the number of replicates was less than 5 (Liao and Wiedmann, 2005). Although the data variation became less with the increase of the number of replicates, the determined mean hardness value remained similar (Liao and Wiedmann, 2005). In this study, the measurements were typically repeated 2–10 times, it is not surprising to see 5–50% variation in hardness at the same peak load, but it is believed that the determined mean hardness value at a certain peak load is representative. Multiple measurements for different locations of a same particle or crystal have indicated that the data reproducibility for the four materials is generally acceptable.

Table 6
Hardness values from this study for single particles at a fixed peak load of ~33 μN and those from previous studies for compacts with a solid fraction of 0.85 using a bulk impact-rebound method

Material	Hardness from this study (GPa)	Hardness from previous studies (GPa)
Sucrose	2.0	0.212 (Mullarney et al., 2003)
Lactose	0.5	0.656 (Narayan and Hancock, 2003)
Ascorbic acid	5.6	0.043 (Mullarney and Hancock, 2004)
Ibuprofen	0.5	0.035, 0.099, 0.161 (Hiestand et al., 1981)

Besides data variation, another important factor that can affect the hardness is the indentation size or peak load. The indentation size effect has been commonly observed in microindentation and nanoindentation for metals (Doerner and Nix, 1986; Gerberich et al., 2002; Swadener et al., 2002; Rodriguez and Gutierrez, 2003; Qian et al., 2005; Durst et al., 2006), indicating that the hardness decreases as the indentation size or peak load increases. It was proposed that the size effect was intrinsically linked to non-uniform deformation and the strain gradient plasticity model was developed using the concept of geometrically necessary dislocations (Fleck et al., 1994; Nix and Gao, 1998). Unlike those previous studies for metals, different extents of indentation size effect were observed for the pharmaceutical materials in this study. For the HPMC film, little or no indentation size or peak load effect on hardness was observed. This observation is consistent with a previous study for polycarbonate and polystyrene thin films (Du et al., 2001). Similarly, no indentation size effect was observed for the ascorbic acid crystal. However, some extents of indentation size or peak load effect were observed for sucrose, ascorbic acid and ibuprofen. Additionally, a previous study for potassium chloride and acetaminophen crystals has also shown different extents of peak load effect on hardness (Liao and Wiedmann, 2005). Therefore, the effects of indentation size or peak load on hardness are probably related to intrinsic properties of the sample. Although it was observed that the hardness decreases with the increase of indentation size or peak load for metals, indentation size or peak load may have different impact on particle hardness for pharmaceutical solids. To better evaluate the indentation size effect, further effort will be needed to reduce data variations.

Since both data variation and effects of indentation size or peak load can affect the particle hardness from AFM nanoindentation, it is important to consider both for quantification and comparison of the particle hardness of different materials. Specifically, the particle hardness should be reported associated with the peak load or contact depth, and multiple measurements at different sample locations should be conducted to obtain representative results and assess data variation. When the particle hardness values of different materials are compared, they should be compared at the same peak load or the same range of the peak loads. A previous studies for potassium chloride and acetaminophen samples plotted the hardness as a function of applied force with measurement variations, and it clearly showed the hardness at different forces and indicated the hardness rank order in a range of applied forces (Liao and Wiedmann, 2005). A similar approach is employed in this study. Fig. 6 plots relationships among hardness, peak load and contact depth. For better comparison, the plots are in logarithmic scales and error bars are included. Fig. 6a shows the hardness as a function of the peak load. The plot clearly indicates that, at the same peak load of the 16–70 μN studied range, the ascorbic acid has the largest hardness among the four materials and the sucrose has the

second largest. The hardness of lactose and ibuprofen appears to be similar by extrapolating the data points of the two samples. For example, at a peak load of ~33 μN, the hardness values for ascorbic acid, sucrose, lactose and ibuprofen are estimated to be 5.6, 2.0, 0.5 and 0.5 GPa, respectively. This hardness order is further confirmed by the correlation between $\log(h_c)$ and $\log(P_{max})$ in Fig. 6b. At the same peak load, the produced contact depth ranks as ascorbic acid < sucrose < lactose ≈ ibuprofen. As a smaller contact depth is expected for a harder material at the same peak load, the order in contact depth is consistent with that in hardness. Therefore, it is concluded that the hardness of the four materials ranks as ascorbic acid > sucrose > lactose ≈ ibuprofen at contact depths from ~40 to 400 nm or peak loads ranging from ~16 to 70 μN.

It is of interest to employ particle mechanical properties to help solid dosage form design. A previous study conducted for sulfathiazole polymorphs tried to relate the tableting performance assessed by an instrumented tableting machine to the mechanical properties measured by nanoindentation. However, little correspondence was found between the macroscopic and microscopic measurements due to the complexity of the tablet compaction (Picker-Freyer et al., 2007). To simplify this complicated correlation issue, only hardness is examined and discussed here. Table 6 summarizes some hardness values from this study for single particles and previous studies for compacts. The particle hardness values from this study were obtained from AFM nanoindentation at a fixed peak load of ~33 μN, while the compact hardness values from previous studies were obtained from a bulk impact-rebound method with a fixed load (the hardness unit was converted to GPa for better comparison). It is not surprising that the results from nanoindentation and impact-rebound method are very different because of large differences in instrumentation, measurement scale, and sample characteristics. Further examination of the hardness values of the four materials in Table 6 shows that the order of particle hardness is almost opposite to that of compact hardness. For example, the ascorbic acid has the largest particle hardness value but the smallest compact hardness. The reverse order of the two data sets is related to intrinsic particle properties and the formation of the compact. When the individual particle of the sample (e.g. ascorbic acid) has a large hardness, the particles do not plastically deform under compression, rather they consolidate through particle rearrangement. The compacts of such samples may be easily indented under the impact of the indenter because the weakly bonded particles can shift around one another, resulting in a small hardness value from the bulk method (Hiestand, 1996; Mullarney and Hancock, 2004). These materials, which have been referred to "special case" material (Hiestand, 1996), usually exhibit poor tableting properties and may need special care for tablet development. Therefore, the particle hardness determined by AFM nanoindentation may help to identify the "special case" materials to aid tablet development. However, it is complicated to relate the particle hardness to compact hardness or tableting performance and will require further study.

5. Conclusions

The hardness of individual particles of various pharmaceutical solids was quantified by AFM nanoindentation. The results show acceptable reproducibility and indicate that the data variation was primarily from the inhomogeneous nature of the samples. Different extents of indentation size or peak load effect on hardness were observed. With consideration of both data variation and indentation size or peak load effect, the hardness of different samples was compared at similar contact depths or peak loads. The hardness ranked as: ascorbic acid > sucrose > lactose ≈ ibuprofen, at contact depths from ~40 to 400 nm or peak loads from ~16 to 70 μN.

Acknowledgement

Helpful discussion and review on this manuscript by Dr. Bruno C. Hancock was greatly appreciated.

References

Amidon, G.E., 1995. Physical and mechanical property characterization of powders. Drugs Pharm. Sci. 70, 281–319.
Belikov, S., Magonov, S., Erina, N., Huang, L., Su, C., Rice, A., Meyer, C., Prater, C., Ginzburg, V., Meyers, G., McIntyre, R., Lakrout, H., 2007. Theoretical modeling and implementation of elastic modulus measurement at the nanoscale using atomic force microscope. J. Phys.: Conf. Ser. 61, 1303–1307.
Bolshakov, A., Pharr, G.M., 1998. Influences of pileup on the measurement of mechanical properties by load and depth sensing indentation techniques. J. Mater. Res. 13, 1049–1058.
Doerner, M.F., Nix, W.D., 1986. A method for interpreting the data from depth-sensing indentation instruments. J. Mater. Res. 1, 601–609.
Du, B., Tsui, O.K.C., Zhang, Q., He, T., 2001. Study of elastic modulus and yield strength of polymer thin films using atomic force microscopy. Langmuir 17, 3286–3291.
Durst, K., Backes, B., Franke, O., Goeken, M., 2006. Indentation size effect in metallic materials: modeling strength from pop-in to macroscopic hardness using geometrically necessary dislocations. Acta Mater. 54, 2547–2555.
Fleck, N.A., Muller, G.M., Ashby, M.F., Hutchinson, J.W., 1994. Strain gradient plasticity: theory and experiment. Acta Metall. Mater. 42, 475–487.
Fraxedas, J., Garcia-Manyes, S., Gorostiza, P., Sanz, F., 2002. Nanoindentation: toward the sensing of atomic interactions. Proc. Natl. Acad. Sci. U.S.A. 99, 5228–5232.
Gerberich, W.W., Tymiak, N.I., Grunlan, J.C., Horstemeyer, M.F., Baskes, M.I., 2002. Interpretations of indentation size effects. J. Appl. Mech. 69, 433–442.
Hancock, B.C., Carlson, G.T., Ladipo, D.D., Langdon, B.A., Mullarney, M.P., 2001. The powder flow and compact mechanical properties of two recently developed matrix-forming polymers. J. Pharm. Pharmacol. 53, 1193–1199.
Hancock, B.C., Clas, S.D., Christensen, K., 2000. Micro-scale measurement of the mechanical properties of compressed pharmaceutical powders. 1: the elasticity and fracture behavior of microcrystalline cellulose. Int. J. Pharm. 209, 27–35.
Hiestand, E.N., 1996. Rationale for and the measurement of tableting indices. Drugs Pharm. Sci. 71, 219–244.
Hiestand, E.N., 1997. Mechanical properties of compacts and particles that control tableting success. J. Pharm. Sci. 86, 985–990.
Hiestand, E.N., Amidon, G.E., Smith, D.P., Tiffany, B.D., 1981. Proceedings Technical Programme: International Powder Bulk Solids Handling, Rosemont, IL, 12–14 May, pp. 383–387.
Hiestand, E.N., Bane Jr., J.M., Strzelinski, E.P., 1971. Impact test for hardness of compressed powder compacts. J. Pharm. Sci. 60, 758–763.
Liao, X., Wiedmann, T.S., 2004. Characterization of pharmaceutical solids by scanning probe microscopy. J. Pharm. Sci. 93, 2250–2258.
Liao, X., Wiedmann, T.S., 2005. Measurement of process-dependent material properties of pharmaceutical solids by nanoindentation. J. Pharm. Sci. 94, 79–92.
Lua, Y.-Y., Cao, X., Rohrs, B.R., Aldrich, D.S., 2007. Surface characterizations of spin-coated films of ethylcellulose and hydroxypropyl methylcellulose blends. Langmuir 23, 4286–4292.
Mullarney, M.P., Hancock, B.C., 2004. Improving the prediction of exceptionally poor tableting performance: an investigation into hiestand's "Special case". J. Pharm. Sci. 93, 2017–2021.
Mullarney, M.P., Hancock, B.C., 2006. Mechanical property anisotropy of pharmaceutical excipient compacts. Int. J. Pharm. 314, 9–14.
Mullarney, M.P., Hancock, B.C., Carlson, G.T., Ladipo, D.D., Langdon, B.A., 2003. The powder flow and compact mechanical properties of sucrose and three high-intensity sweeteners used in chewable tablets. Int. J. Pharm. 257, 227–236.
Narayan, P., Hancock, B.C., 2003. The relationship between the particle properties, mechanical behavior, and surface roughness of some pharmaceutical excipient compacts. Mater. Sci. Eng., A A355, 24–36.
Nix, W.D., Gao, H., 1998. Indentation size effects in crystalline materials: a law for strain gradient plasticity. J. Mech. Phys. Solids 46, 411–425.
Oliver, W.C., Pharr, G.M., 1992. An improved technique for determining hardness and elastic modulus using load and displacement sensing indentation experiments. J. Mater. Res. 7, 1564–1583.
Perkins, M., Ebbens, S.J., Hayes, S., Roberts, C.J., Madden, C.E., Luk, S.Y., Patel, N., 2007. Elastic modulus measurements from individual lactose particles using atomic force microscopy. Int. J. Pharm. 332, 168–175.
Pharr, G.M., 1998. Measurement of mechanical properties by ultra-low load indentation. Mater. Sci. Eng., A A253, 151–159.
Picker-Freyer, K.M., Liao, X., Zhang, G., Wiedmann, T.S., 2007. Evaluation of the compaction of sulfathiazole polymorphs. J. Pharm. Sci. 96, 2111–2124.
Podczeck, F., 2001. Investigations into the fracture mechanics of acetylsalicylic acid and lactose monohydrate. J. Mater. Sci. 36, 4687–4693.
Qian, L., Li, M., Zhou, Z., Yang, H., Shi, X., 2005. Comparison of nano-indentation hardness to microhardness. Surf. Coat. Technol. 195, 264–271.
Ramos, K.J., Bahr, D.F., 2007. Mechanical behavior assessment of sucrose using nanoindentation. J. Mater. Res. 22, 2037–2045.
Ridgway, K., Shotten, E., Glasby, J., 1969. Hardness and elastic modulus of some crystalline pharmaceutical materials. J. Pharm. Pharmacol. 21, 19S–23S.

Rodriguez, R., Gutierrez, I., 2003. Correlation between nanoindentation and tensile properties influence of the indentation size effect. Mater. Sci. Eng. A 361, 377–384.

Rowe, R.C., Roberts, R.J., 1995. The mechanical properties of powders. Adv. Pharm. Sci. 7, 1–62.

Sun, C., Grant, D.J.W., 2001. Influence of crystal shape on the tableting performance of L-lysine monohydrochloride dihydrate. J. Pharm. Sci. 90, 569–579.

Swadener, J.G., George, E.P., Pharr, G.M., 2002. The correlation of indentation size effect experiments with pyramidal and spherical indenters. Mater. Res. Soc. Symp. Proc. 695, 451–456.

Taylor, L.J., Papadopoulos, D.G., Dunn, P.J., Bentham, A.C., Dawson, N.J., Mitchell, J.C., Snowden, M.J., 2004a. Predictive milling of pharmaceutical materials using nanoindentation of single crystals. Org. Process Res. Dev. 8, 674–679.

Taylor, L.J., Papadopoulos, D.G., Dunn, P.J., Bentham, A.C., Mitchell, J.C., Snowden, M.J., 2004b. Mechanical characterization of powders using nanoindentation. Powder Technol. 143–144, 179–185.

Vanlandingham, M.R., McKnight, S.H., Palmese, G.R., Elings, J.R., Huang, X., Bogetti, T.A., Eduljee, R.F., Gillespie Jr., J.W., 1997. Nanoscale indentation of polymer systems using the atomic force microscope. J. Adhes. 64, 31–59.